



The First Photometric Study of AH Mic Contact Binary System

Atila Poro¹ , M. G. Blackford² , S. Ranjbar Salehian³ , E. Jahangiri³ , M. Samiei Dastjerdi³ , M. Gozarandi³ ,
R. Karimi^{3,4} , T. Madayen⁵ , E. Bakhshi^{3,6} , and F. Hedayati³ 

¹ Astronomy Department of the Raderon Lab., BC, Burnaby, Canada; astronomydep@raderonlab.ca, poroatila@gmail.com

² Variable Stars South (VSS), Congarinni Observatory, Congarinni, NSW, 2447, Australia

³ Binary Systems of South and North (BSN) Project, Contact Systems Department, Iran

⁴ Department of Physics, Kharazmi University, Tehran, Iran

⁵ Astronomy and Astrophysics Department, University of Toronto, Toronto, Canada

⁶ Department of Physics, Institute for Advanced Studies in Basic Sciences (IASBS), Zanjan, Iran

Received 2022 January 26; revised 2022 March 22; accepted 2022 April 1; published 2022 April 29

Abstract

The first multi-color light curve analysis of the AH Mic binary system is presented. This system has very few past observations from the southern hemisphere. We extracted the minima times from the light curves based on the Markov Chain Monte Carlo (MCMC) approach and obtained a new ephemeris. To provide modern photometric light curve solutions, we used the Physics of Eclipsing Binaries (PHOEBE) software package and the MCMC approach. Light curve solutions yielded a system temperature ratio of 0.950, and we assumed a cold starspot for the hotter star based on the O'Connell effect. This analysis reveals that AH Mic is a W-subtype W UMa contact system with a fill-out factor of 21.3% and a mass ratio of 2.32. The absolute physical parameters of the components are estimated by using the Gaia Early Data Release 3 (EDR3) parallax method to be $M_h(M_\odot) = 0.702(26)$, $M_c(M_\odot) = 1.629(104)$, $R_h(R_\odot) = 0.852(21)$, $R_c(R_\odot) = 1.240(28)$, $L_h(L_\odot) = 0.618(3)$ and $L_c(L_\odot) = 1.067(7)$. The orbital angular momentum of the AH Mic binary system was found to be 51.866(35). The components' positions of this system are plotted in the Hertzsprung–Russell diagram.

Key words: photometry – binary stars – individual (AH Mic)

1. Introduction

Each component of a contact binary system has its own Roche lobe, with the inner and outer critical surfaces sharing a common envelope. These stars are generally late type F, G or K type stars. The majority of contact systems are solar-type dwarfs with active stellar populations, as evidenced by their asymmetric light curves and spectral line profiles.

Contact binaries typically have orbital periods of less than one day, and the Zhang & Qian (2020) investigation found that the lower limit of orbital period is 0.15 day. The orbital period frequently varies over time, due to mass transfer from one component to the other, as well as mass and angular momentum loss from the binary system. Although, according to the Latković et al. (2021) study, systems with orbital periods of more than 0.5 day and temperatures greater than 7000 K probably have radiative envelopes and should not be classified as W Ursae Majoris (W UMa)-type contact binaries.

Contact binaries are debatable in terms of mass, and the lower limit of mass ratio for these systems is presently under investigation (e.g., Li & Zhang 2006; Arbutina 2007; Yang & Qian 2015). Additionally, since many investigations lack a spectroscopic method, determining the mass ratio is a challenging issue.

W UMa-type contact systems (EW) are classified into two categories, W-type and A-type, based on their properties. The mass ratio in A-subtype systems is often less than 0.5, showing weak or moderate activity. In W-subtype systems the less massive component is hotter and the period changes continuously over time (Binnendijk 1970). In comparison with the W-subtypes, A-subtype systems are earlier spectral types with higher mass and luminosity.

The purpose of this study is to present the first light curve analysis of the AH Mic binary system and determine its properties. AH Mic is a binary system from the southern hemisphere with a range of apparent magnitude of $V = 12.85\text{--}13.45$ and an orbital period of 0.3243344 day (Watson et al. 2006). In all the available catalogs, this binary system is classified as an EW-type system. This paper is arranged as follows: Section 2 contains information about the multi-color photometric observations from an Australian observatory as well as a data reduction technique. Section 3 explains how to extract our times of minima, compile minima collection times from literature and compute a new ephemeris. The Physics of Eclipsing Binaries (PHOEBE) Python code and the Markov Chain Monte Carlo (MCMC) approach were used to study the light curves of the AH Mic system, and the

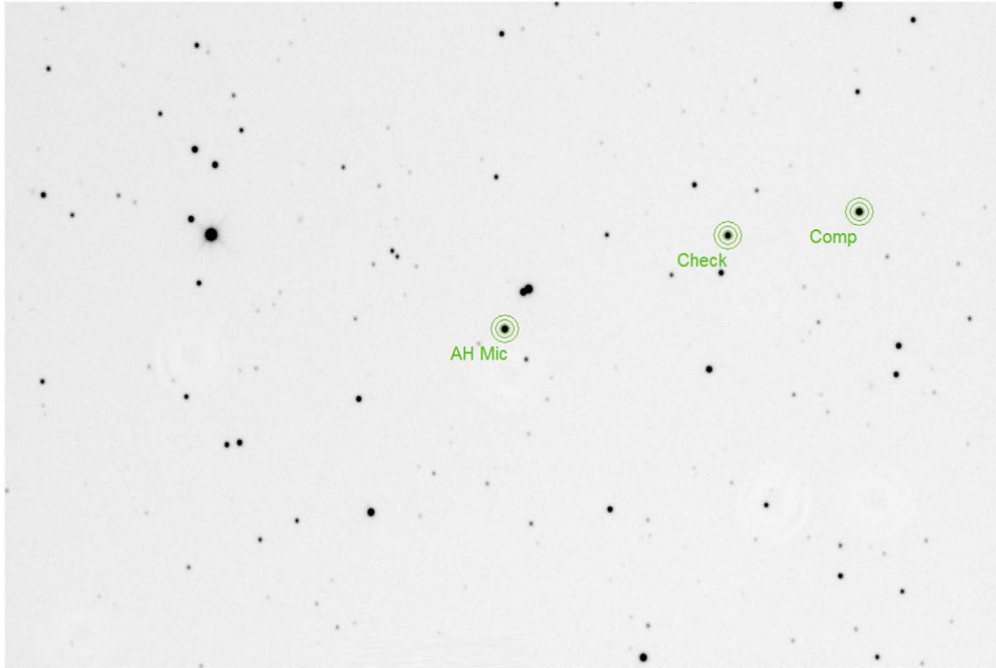


Figure 1. AH Mic, comparison star and check star field-of-view. The circles are solely used to mark the position of each star, which is indicated by bigger rings.

absolute parameters are obtained in Section 4. Section 5 has a summary and conclusion.

2. Observation and Data Reduction

AH Mic (R.A. 21 04 57.8280, decl. $-40\ 33\ 06.084$ (J2000)) was observed for six nights in August and September 2020 with a GSO 14 inch $f/8$ Ritchey-Chretien telescope at the Congarinni Observatory in Australia ($152^{\circ}52'$ East and $30^{\circ}44'$ South). The data were taken using an SBIG STT3200-ME CCD camera (2184×1510 pixels, $6.8\ \mu\text{m}$ square) with 2×2 binning and a CCD temperature of -15°C . These observations were made utilizing the Astrodon Johnson-Cousins $BVRI$ standard filters. The exposure time of these observations for BI filters is 120 s and for VR filters is 60 s. GSC 7969-723 was selected as a comparison star and GSC 7969-1170 was chosen as a check star with an appropriate apparent magnitude in comparison to AH Mic. The comparison star was found at R.A. $21^{\text{h}}\ 04^{\text{m}}\ 49^{\text{s}}.91976$ (J2000), decl. $-40^{\circ}39'42''.8868$ (J2000) with a $V = 12.831$ mag, while the check star was located at R.A. $21^{\text{h}}\ 04^{\text{m}}\ 50^{\text{s}}.96544$ (J2000), decl. $-40^{\circ}37'18''.0120$ (J2000) with a $V = 13.285$ mag, based on the AAVSO Photometric All Sky Survey Data Release 9 (APASS9) catalog. Figure 1 features the observed field-of-view for AH Mic with the comparison and check stars.

During the observations, a total of 1417 images was acquired. The CCD image processing was done with MaxIm DL software, which included dark, bias and flat-field corrections (George 2000). The airmass decreases the flux of stars when light passes through the Earth's atmosphere. We estimated the airmass based

on observatory coordinates and the position of the star in the sky during the observations (Hiltner 1962). Finally, we relied on the AstroImageJ (AIJ) software to normalize all of the ground-based data (Collins et al. 2017) and apply airmass.⁷

3. New Ephemeris Calculation

We extracted the nine times of minima in the light curves, four of which are the primary minima. We used models based on the Gaussian and Cauchy distributions to find the times of minima and the MCMC sampling methods to estimate the uncertainty of the values (Poro et al. 2021). The Python code for this extraction is implemented using the PyMC3 package (Salvatier et al. 2016). All times of minimum are expressed in the Barycentric Julian Date in the Barycentric Dynamical Time (BJD_{TDB}), and Table 1 lists all CCD times of minima with their uncertainties for the AH Mic system.

$O - C$ variations are the differences between observed mid-eclipse times (O) and their calculated values (C) based on a reference ephemeris. An observable trend in $O - C$ is caused by various factors and effects. Due to the small number of minimum times and the short interval of observation (2013–2020), only a linear fit can be considered for the AH Mic system. We fitted a line to all times of minima to calculate a new ephemeris based on the MCMC approach using the emcee package in Python (Foreman-Mackey et al. 2013) as depicted in Figure 2.

⁷ This study's data (after data reduction) are available in four filters as a supplement file.

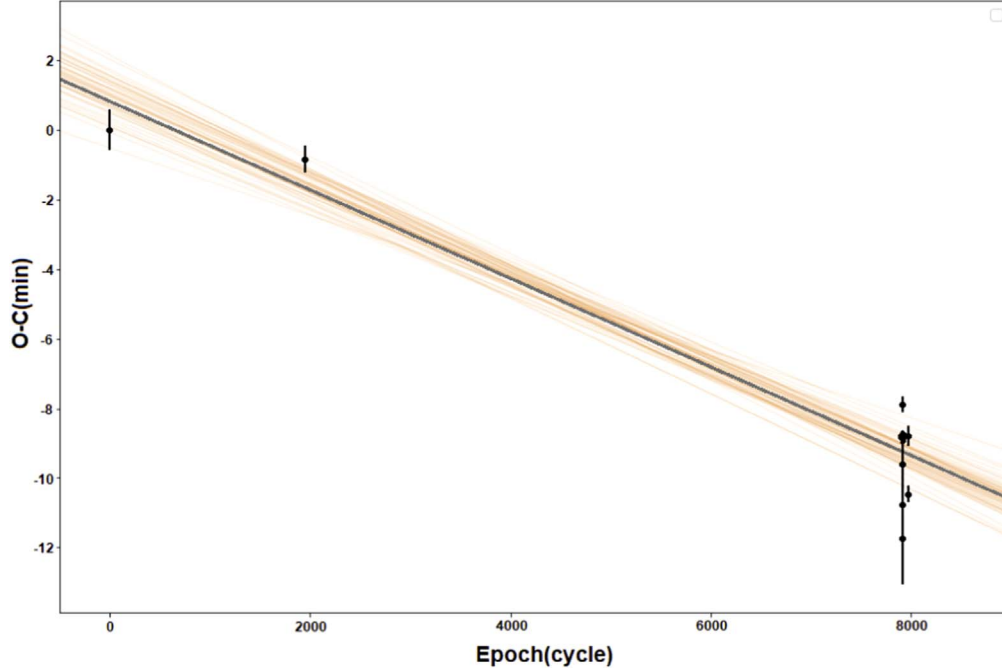


Figure 2. The $O - C$ diagram of the AH Mic system.

Table 1
Available CCD Times of Minima for AH Mic

Min.(BJD _{TDB})	Error	Epoch	$O - C$	Reference
2456523.00509	0.000 40	0	0	Diethelm (2014)
2457154.80792	0.000 27	1948	-0.0006	Jayasinghe et al. (2019)
2459108.91600	0.000 17	7973	-0.0073	This study
2459089.94354	0.000 10	7914.5	-0.0062	This study
2459090.10578	0.000 07	7915	-0.0061	This study
2459090.91664	0.000 08	7917.5	-0.0061	This study
2459091.07740	0.000 13	7918	-0.0075	This study
2459091.24157	0.000 16	7918.5	-0.0055	This study
2459092.05120	0.000 50	7921	-0.0067	This study
2459092.21189	0.000 92	7921.5	-0.0081	This study
2459109.07933	0.000 20	7973.5	-0.0061	This study

We determined a new ephemeris for primary minimum as follows

$$\text{BJD}_{\text{TDB}}(\text{MinI.}) = (2456523.00559 \pm 0.00068) + (0.32433351 \pm 0.00000009) \times E. \quad (1)$$

4. Photometric Solutions

4.1. Light Curve Analysis

We utilized the latest Python version of the PHOEBE software package (2.3.58) to model the light curves of the AH

Mic binary system. We employed PHOEBE along with the emcee package (Foreman-Mackey et al. 2013), with the MCMC approach for more precision in modeling, output results and uncertainties. We applied 32 walkers and 1000 iterations to each walker in the MCMC approach. The PHOEBE and MCMC approach then searched for the temperature ratio, orbital inclination and mass ratio. The bolometric albedo and gravity-darkening coefficients were assumed to be $g_h = g_c = 0.32$ (Lucy 1967) and $A_h = A_c = 0.5$ (Ruciński 1969) respectively. The stellar atmosphere was modeled using the Castelli & Kurucz (2004) method, and the limb-darkening coefficients were employed as free parameters in PHOEBE. Different methods were used to determine the effective temperature for the hotter component as a fixed parameter. (1) The temperature from Gaia Data Release 2 (DR2)⁸ for the AH Mic system is $5381^{+(74)}_{-(51)}$ K; (2) the result of the $B - V$ index obtained from this work's light curves is 0.73 ± 0.04 after calibration (Høg et al. 2000) and consequently we found the effective temperature $5470^{+(111)}_{-(119)}$ K according to the Flower (1996) study; (3) the effective temperature from the result of the Poro et al. (2022) analysis of the relationship between orbital period and the primary (hotter) temperature for contact systems is $5681^{+(81)}_{-(80)}$ K. We chose Gaia DR2's temperature as a fixed parameter for the hotter star. In the continuation, we performed the initial light curve analysis. Then, based on the following equations from

⁸ <https://gea.esac.esa.int/archive/>

Table 2
Photometric Solutions of AH Mic

Parameter	Result
T_h (K)	$5550^{+(74)}_{-(51)}$
T_c (K)	$5274^{+(40)}_{-(63)}$
q	$2.32^{+(8)}_{-(4)}$
$\Omega_h = \Omega_c$	$5.57^{+(48)}_{-(13)}$
i°	$75.91^{+(79)}_{-(35)}$
f	$0.213^{+(35)}_{-(12)}$
l_h/l_{tot}	0.381(2)
l_c/l_{tot}	0.619(2)
$r_{h(\text{mean})}$	0.324(2)
$r_{c(\text{mean})}$	0.470(2)
Phase shift	-0.005(1)
Colatitude (deg)	90(2)
Longitude (deg)	274(1)
Radius (deg)	20(1)
$T_{\text{spot}}/T_{\text{star}}$	0.91(2)

the Kjurkchieva et al. (2018) study, we calculated the temperatures and generated the final photometric light curve solutions:

$$T_1 = T_m + \frac{c\Delta T}{c+1}, \quad (2)$$

$$T_2 = T_1 - \Delta T, \quad (3)$$

where ΔT is the temperature difference between the two stars, and c is l_2 divided by l_1 .

The *BVRI* light curves of the AH Mic system are asymmetric in the maxima. This shows that the O’Connell effect (O’Connell 1951) is present in this system, as Max II is brighter than Max I. We employed a stellar spot model during the light curve solution in all used filters, and we found that assuming a cool starspot model on the hotter component leads to the appropriate solutions for all *BVRI* light curves (Table 2). Table 3 displays the characteristic properties of the AH Mic light curves, with the difference in maxima in each filter displayed in the first row. Therefore, the *B* filter had the highest difference between the levels of maximum light and the depths of the minima, while the *R* filter had the least. This is expected because of the induced changes in the magnetic activity.

Table 2 shows the results of the light curve analysis, whereas Figure 3 displays the observational and theoretical light curves of our modeling. Figure 4 depicts the 3D view and geometrical structure of the AH Mic binary system.

4.2. Absolute Parameters

The Gaia Early Data Release 3 (EDR3) parallax method can be applied to estimate the absolute parameters when only photometric data are available. Several elements from observational and light curve analysis are used in the computations, despite the fact that the

Table 3
Characteristic Parameters of the Observational Light Curves in *BVRI* Filters

Light Curve	$\Delta B^{(\text{mag.})}$	$\Delta V^{(\text{mag.})}$	$\Delta R^{(\text{mag.})}$	$\Delta I^{(\text{mag.})}$
Max I–Max II	0.021	0.020	0.015	
Max I–Min II	-0.479	-0.494	-0.472	-0.468
Max I–Min I	-0.618	-0.613	-0.574	-0.552
Min I–Min II	0.139	0.119	0.102	0.084

Gaia EDR3 parallax has high accuracy for this estimation. Recent investigations have made some corrections to the Gaia EDR3 parallax (e.g., Lindegren et al. 2021; Ren et al. 2021). The range of these corrections appears to include the value of observational and light curve solution uncertainties (Poro et al. 2022).

Therefore, in order to properly estimate the absolute parameters of the stars in the AH Mic binary system, we relied on the Gaia EDR3 parallax method. This is a well-known method, which is fully described in the Poro et al. (2022) study.

To perform the estimation, we first obtained the absolute magnitude (M_V) of the system using the maximum light of apparent magnitude $V_{\text{max}} = 12.79(5)$ from our observation, the star’s distance from Gaia EDR3 $d_{(\text{pc})} = 470.2(6.5)$ and the extinction coefficient $A_V = 0.08$ from the Schlafly & Finkbeiner (2011) study. Then, by utilizing the values of l_h/l_{tot} and l_c/l_{tot} from the light curve solutions, we obtained the M_V value of each of the components. In addition, the bolometric magnitude M_{bol} values of each star were obtained using $\text{BC}_h = -0.133$ and $\text{BC}_c = -0.199$. Furthermore, the luminosity (L) values were estimated and the radius values of each star were obtained using the temperature of the stars from the light curve solutions. The semimajor axis of the system was also determined by utilizing the $a = R/r_{(\text{mean})}$ equation. According to Kepler’s third law, the value of $M_h + M_c$ could be estimated using the semimajor axis and the orbital period of the system. Moreover, the masses of the hotter and cooler stars were determined using the value of mass ratio.

To estimate the uncertainties using mass ratio and temperature from light curve analysis, we used the average value of uncertainties rather than the upper and lower ranges. The results of estimating the absolute parameters for the AH Mic system are shown in Table 4.

For comparison, we calculated absolute magnitude of the system using the orbital period-luminosity calibration of Rucinski (2006)

$$M_V = (-1.5) - 12 \log P. \quad (4)$$

The result of relation (4) shows $M_V^{(\text{mag.})} = 4.37$, while in our estimation $M_V^{(\text{mag.})} = 4.349(10)$ which indicates relatively close values.

5. Summary and Conclusion

Observations were made on the *BVRI* filters for the AH Mic binary system in the southern hemisphere. The MCMC

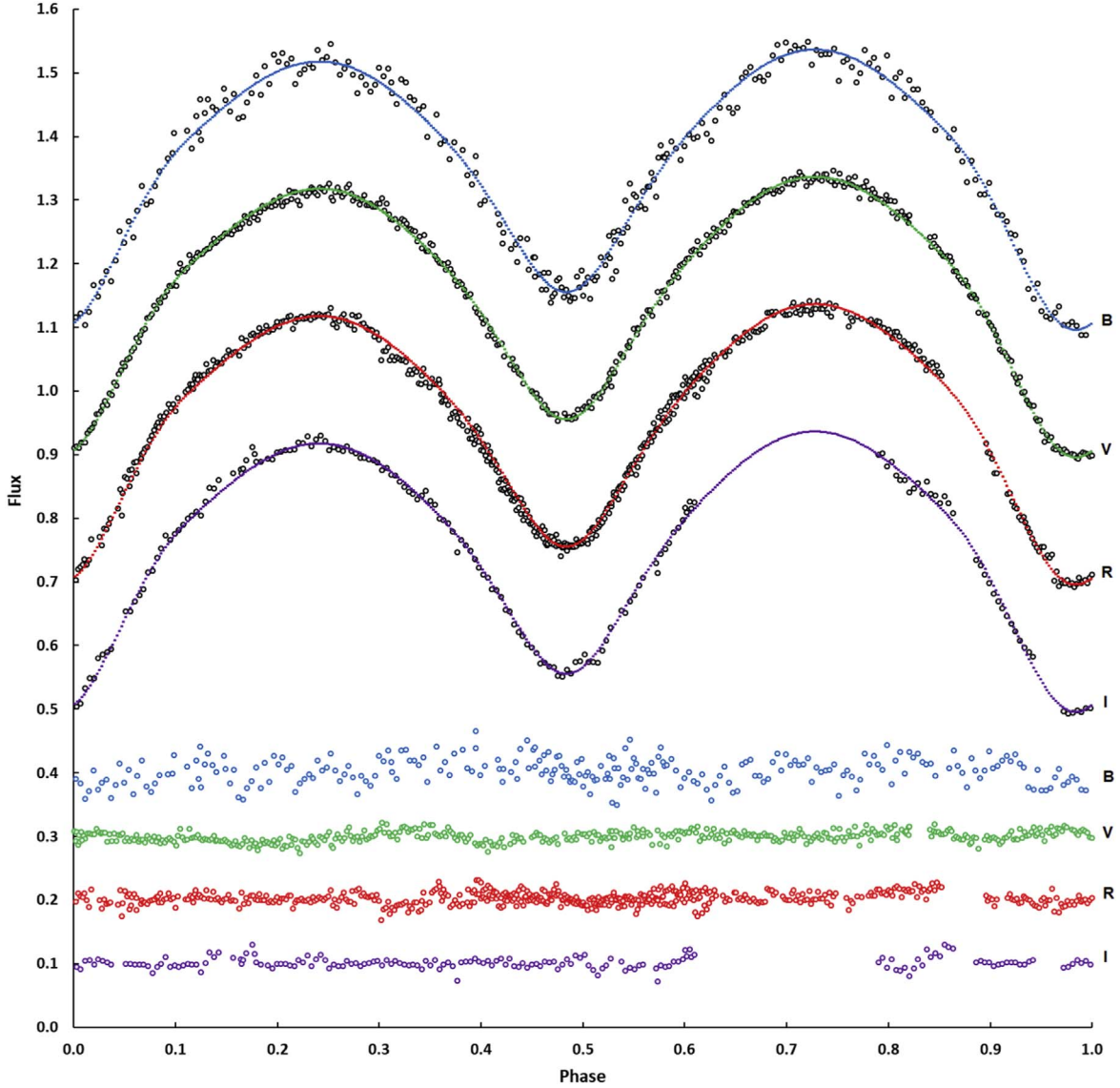


Figure 3. The observed light curves of AH Mic (black dots), and synthetic light curves obtained from light curve solutions and residuals are plotted, with respect to orbital phase, shifted arbitrarily in the relative flux.

Table 4
Estimation of Absolute Parameters of AH Mic Binary System

Parameter	Hotter Star	Cooler Star
$M (M_{\odot})$	0.702(26)	1.629(104)
$R(R_{\odot})$	0.852(21)	1.240(28)
$L(L_{\odot})$	0.618(3)	1.067(7)
M_{bol} (mag.)	5.263(5)	4.670(7)
$\log(g)$ (cgs)	4.423(5)	4.463(8)
$a (R_{\odot})$	2.634(48)	

approach was applied to extract the times of minima for our light curves, and the times of minima were also collected from previous observations. Accordingly, we presented a new ephemeris. The first light curve analysis of the AH Mic system was done in this work, which was performed using the latest version of the PHOEBE Python code and the MCMC approach. To estimate the system's absolute parameters, we relied on the Gaia EDR3 parallax method, and the rest of the parameters were calculated using the observational parameters and the light curve solutions from this study.

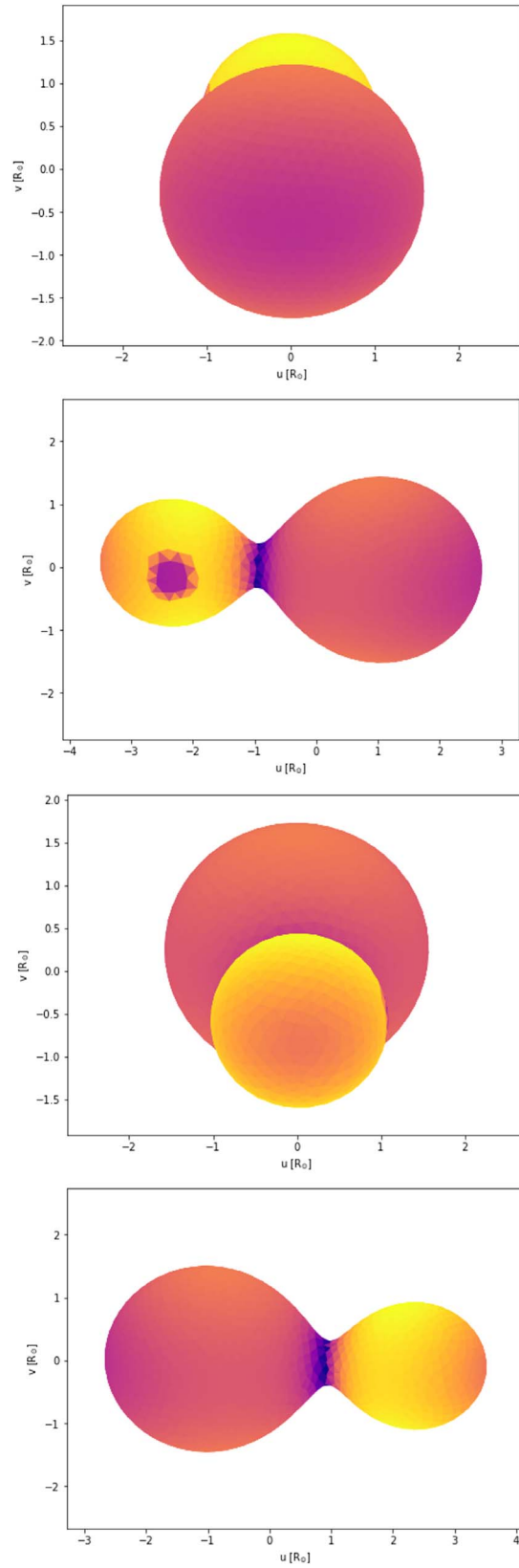


Figure 4. The positions of the components of AH Mic.

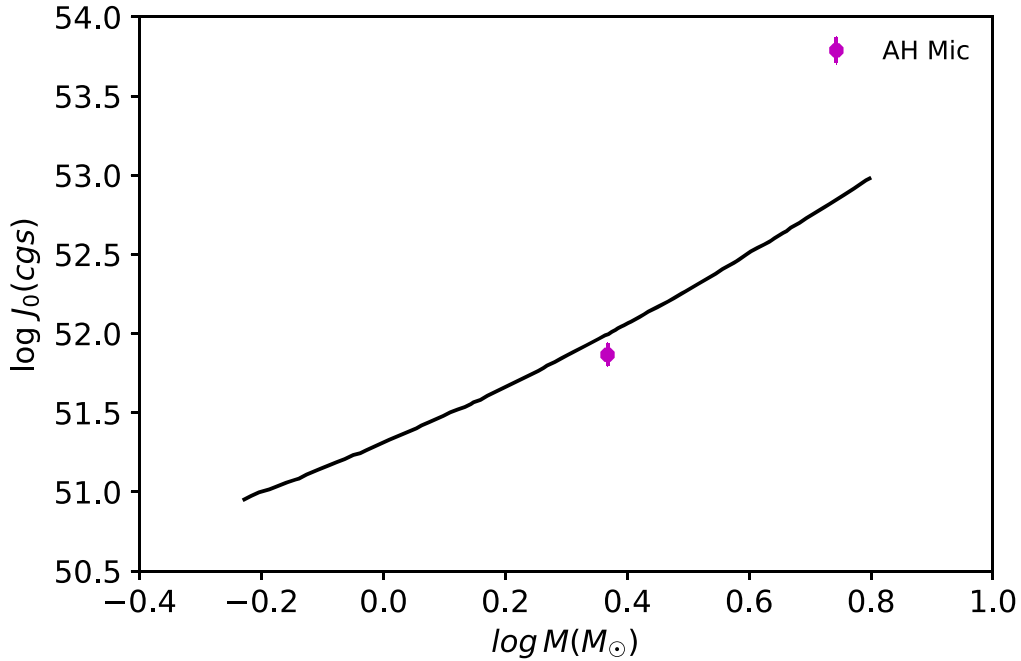


Figure 5. The location of AH Mic on the $\log J_0$ – $\log M$ diagram. Detached and contact binary systems are separated by a quadratic border line. The quadratic line is based on a study by Eker et al. (2006).

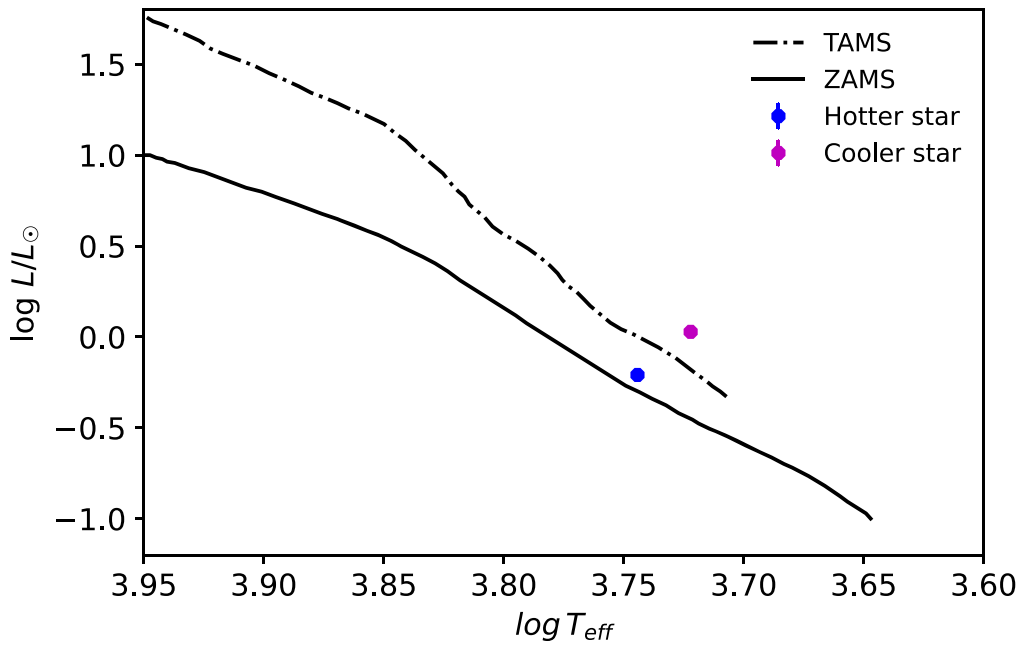


Figure 6. The hotter star and cooler star in the AH Mic system are shown on the H-R diagram.

We fixed the Gaia EDR3 temperature for the hotter component at first, and obtained the cooler component temperature from light curve solutions. This temperature is from the combination of both stars in the system. So, using Equation (2), we obtained the final

temperature values of each star. The temperature difference between the two components is 276 K. According to Allen’s table (Cox 2000), these temperatures indicate that the spectral types of the hotter and cooler components are G5 and G8 respectively.

The mass ratio is an important parameter for contact binaries and it is determined through q -search when there are just photometric observations. The mass ratio in this study was determined using a method based on the MCMC approach. The reliable value of mass ratio through photometric light curve analysis is still under many investigations to approach the accuracy of this value using the spectroscopy method. However, investigations have been conducted, one of which is based on the Machine Learning methods implementing the Multi-Layer Perceptron (MLP) regression model and was carried out by the Poro et al. (2022) study. According to this method, we find the estimated range of mass ratio for AH Mic to be 0.408 to 0.572 with a mean of 0.485, which includes our calculated mass ratio of 0.431 from the light curve solutions. It is worth mentioning that the q specified in the Poro et al. (2022) study is the ratio of the less massive star mass to the more massive star mass, hence q is never more than unity.

The orbital angular momentum (J_0) of the AH Mic system was calculated, and its location is displayed on the $\log J_0 - \log M$ diagram (Figure 5). The value of $\log J_0$ of AH Mic was obtained to be 51.866 ± 0.035 . The diagram shows that this system is in a region of contact binary systems.

The Hertzsprung–Russell (H-R) diagram depicts the evolutionary state of the components (Figure 6). The cooler star (which is more massive) has already evolved away from the terminal-age main sequence (TAMS in Figure 6), and the hotter star is in the main sequence belt and above the zero-age main sequence (ZAMS in Figure 6). According to the value of the mass ratio, the fill-out factor, inclination and location of components on the H-R diagram, AH Mic follows the general pattern of W-type W UMa systems.

Acknowledgments

This manuscript was prepared based on the Binary Systems of the South and North Project (<http://bsnp.info>). The goal of the project is to investigate contact binary systems in the northern and southern hemispheres using observatories throughout the world.

We utilized the latest version of Gaia EDR3 (<http://www.cosmos.esa.int/gaia>) data from the European Space Agency (ESA) mission Gaia in this study. This work has made use of the SIMBAD database, operated by CDS, Strasbourg, France. Also, we used the latest version of PHOEBE related to this project website (<http://phoebe-project.org/>). PHOEBE is

funded in part by the National Science Foundation (NSF 1 517 474, 1 909 109) and the National Aeronautics and Space Administration (NASA 17-ADAP17-68).

ORCID iDs

Atila Poro  <https://orcid.org/0000-0002-0196-9732>
 M. G. Blackford  <https://orcid.org/0000-0003-0524-2204>
 S. Ranjbar Salehian  <https://orcid.org/0000-0002-5223-1332>
 E. Jahangiri  <https://orcid.org/0000-0002-1576-798X>
 M. Samiei Dastjerdi  <https://orcid.org/0000-0002-7502-3907>
 M. Gozarandi  <https://orcid.org/0000-0002-5131-6801>
 R. Karimi  <https://orcid.org/0000-0003-2295-0499>
 T. Madayen  <https://orcid.org/0000-0002-2653-3281>
 E. Bakhshi  <https://orcid.org/0000-0002-8782-6045>
 F. Hedayati  <https://orcid.org/0000-0003-0925-6806>

References

- Arbutina, B. 2007, *MNRAS*, **377**, 1635
 Binnendijk, L. 1970, *VA*, **12**, 217
 Castelli, F., & Kurucz, R. L. 2004, *A&A*, **419**, 725
 Collins, K. A., Kielkopf, J. F., Stassun, K. G., & Hessman, F. V. 2017, *AJ*, **153**, 77
 Cox, A. N. 2000, *Allen's Astrophysical Quantities* (New York: AIP Press)
 Diethelm, R. 2014, *IBVS*, **6093**, 1
 Eker, Z., Demircan, O., Bilir, S., & Karataş, Y. 2006, *MNRAS*, **373**, 1483
 Flower, P. J. 1996, *ApJ*, **469**, 355
 Foreman-Mackey, D., Hogg, D. W., Lang, D., & Goodman, J. 2013, *PASP*, **125**, 306
 George, D. B. 2000, *IAPPP*, **79**, 2
 Hiltner, W. A. 1962, *Astronomical Techniques*
 Høg, E., Fabricius, C., Makarov, V. V., et al. 2000, *A&A*, **357**, 367
 Jayasinghe, T., Stanek, K. Z., Kochanek, C. S., et al. 2019, *MNRAS*, **486**, 1907
 Kjurkchieva, D. P., Dimitrov, D. P., Ibryamov, S. I., & Vasileva, D. L. 2018, *PASA*, **35**, e008
 Latković, O., Čeki, A., & Lazarević, S. 2021, *ApJS*, **254**, 10
 Li, L., & Zhang, F. 2006, *MNRAS*, **369**, 2001
 Lindegren, L., Bastian, U., Biermann, M., et al. 2021, *A&A*, **649**, A4
 Lucy, L. B. 1967, *ZAp*, **65**, 89
 O'Connell, D. J. K. 1951, *PRCO*, **2**, 85
 Poro, A., Davoudi, F., Alicavus, F., et al. 2021, *astL*, **47**, 402
 Poro, A., Sarabi, S., Zamanpour, S., et al. 2022, *MNRAS*, **510**, 5315
 Ren, F., Chen, X., Zhang, H., et al. 2021, *ApJL*, **911**, L20
 Ruciński, S. M. 1969, *AcA*, **19**, 245
 Ruciński, S. M. 2006, *MNRAS*, **368**, 1319
 Salvatier, J., Wieckia, T. V., & Fonnesbeck, C. 2016, *PyMC3: Python Probabilistic Programming Framework*, *Astrophysics Source Code Library*, [ascl:1610.016](https://arxiv.org/abs/1610.016)
 Schlafly, E. F., & Finkbeiner, D. P. 2011, *ApJ*, **737**, 103
 Watson, C. L., Henden, A. A., & Price, A. 2006, *SASS*, **25**, 47
 Yang, Y.-G., & Qian, S.-B. 2015, *AJ*, **150**, 69
 Zhang, X.-D., & Qian, S.-B. 2020, *MNRAS*, **497**, 3493